

## First-principles study of the stability of atomic Ag lines epitaxial to self-assembled Bi nanolines

This article has been downloaded from IOPscience. Please scroll down to see the full text article.

2007 J. Phys.: Condens. Matter 19 266213

(<http://iopscience.iop.org/0953-8984/19/26/266213>)

View [the table of contents for this issue](#), or go to the [journal homepage](#) for more

Download details:

IP Address: 129.252.86.83

The article was downloaded on 28/05/2010 at 19:37

Please note that [terms and conditions apply](#).

# First-principles study of the stability of atomic Ag lines epitaxial to self-assembled Bi nanolines

**H Koga and T Ohno**

Computational Materials Science Centre (CMSC), National Institute for Materials Science (NIMS), 1-2-1 Sengen, Tsukuba, Ibaraki 305-0047, Japan

E-mail: [koga.hiroaki@nims.go.jp](mailto:koga.hiroaki@nims.go.jp) and [ohno.takahisa@nims.go.jp](mailto:ohno.takahisa@nims.go.jp)

Received 28 February 2007, in final form 20 April 2007

Published 14 June 2007

Online at [stacks.iop.org/JPhysCM/19/266213](http://stacks.iop.org/JPhysCM/19/266213)

## Abstract

The stability of single-atom-wide Ag lines epitaxial to a Bi nanoline (a double line of Bi dimers self-assembled on the Si(001) surface) is examined from first principles. The lattice-matched Ag line, which has a coincident-site lattice (CSL) relationship with the Bi nanoline, is found more stable than pseudomorphic ones such as monomer and dimer lines. The greater stability of the single-row CSL line against the double-row one indicates the feasibility of single-row lines. The greater stability of the triple-row line however suggests that the single-row lines should be grown under kinetically controlled conditions.

(Some figures in this article are in colour only in the electronic version)

## 1. Introduction

Atomic-scale nanowires [1] are intensively studied because of their unusual physical properties and, in particular, in order to use them as conducting wires connecting nanoscale devices. Preparation of such nanowires requires the finest control over the behaviour of atoms. One approach is scanning-probe lithography; for example, a line of Si dangling bonds can be created on the H-terminated Si(001) surface by desorbing H atoms with a voltage pulse applied to the probe [2–5]. This dangling bond line can then be used as a template in growing nanowires of elements such as Ga [6, 7] and Ag [8]. Alternatively, self-assembled nanostructures can be used as templates. As such a template, the self-assembled Bi nanoline [9, 10] prepared on the Si(001) surface is particularly promising, because it has a well-defined atomic structure [11] (two Bi dimer lines attached to a surface line defect) extending over 500 nm. According to a recent experiment [12], indium deposited on the surface reacted with the Bi nanolines, forming zigzag chains of In and Bi [13]. Moreover, Ag adsorbed preferentially on the Bi nanolines [14], although the growth of Ag nanowires has not been accomplished. (These experiments [12, 14] use ammonia to passivate the Si(001) surface against metal adsorption.) In addition, a nanowire grown on the Bi nanoline may have interesting physical properties: a density functional theory

(DFT) calculation [15] has predicted a magnetic half-metal behaviour for the one-dimensional array of Fe atoms adsorbed on the Bi nanoline.

To theoretically support the template effect of the Bi nanoline, our previous DFT study [16] has examined the behaviour of a single Ag atom adsorbed on the H-terminated Si(001) surface featuring Bi nanolines. The calculation indicates that the Ag atom incident on the H-terminated Si(001) surface rapidly migrates to a Bi nanoline (barrier  $\sim 0.14$  eV), enters its Bi–Si back-bond (gaining 0.7 eV), and then migrates along the nanoline, moving through back-bonds (barrier  $\sim 0.33$  eV). (The barriers cited in this paper are from [16].) The calculation thus confirms that Ag adsorbs preferentially on the Bi nanoline. More important, the trapping of the Ag atoms in the back-bonds of the Bi nanoline implies the possibility of atomic Ag lines growing there.

In this first-principles study, we therefore examine the stability of Ag lines epitaxial to the Bi nanoline and ascertain their feasibility. We find that the single-row, lattice-matched Ag line, which has a coincident-site lattice (CSL) relationship with the Bi nanoline, is particularly stable. This paper is organized as follows. The calculation methods and models are explained in section 2. The calculation results are presented and discussed in section 3: we first discuss the Ag lines on the exterior of the Bi nanoline (section 3.1) and then those on the interior (section 3.2). In addition to those interior lines growing on one branch of the Bi nanoline (section 3.2.1), we examine double lines growing on both branches (section 3.2.2). Conclusions are given in section 4. A related calculation on thick Ag nanowires is presented elsewhere [17].

## 2. Method

The method and models used in the present calculation are similar to those used in our previous study [16, 17]. The optimized geometries and their energies are obtained in a DFT [18, 19] plane-wave pseudopotential [20, 21] calculation within the generalized gradient approximation (GGA) [22]<sup>1</sup>. The plane-wave cut-off energy is 16 Ryd for wavefunctions and 196 Ryd for charge density.

The slab model of the Bi nanoline surface (figure 1) is derived from a six-layer Si(001) slab terminated in H at the bottom. The two Bi dimer lines constituting the Bi nanoline are attached to a hexagonal Si core surrounded by five- and seven-membered rings [11] (figure 1(b)). The area of the surface outside the Bi nanoline is in the monohydride structure. Two classes of Ag lines are examined: first, pseudomorphic lines where Ag occupies the back-bond sites (figure 1); second, the CSL line where eight Ag atoms match three Bi dimers. The CSL line is lattice matched to the Bi nanoline, that is, close to the bulk Ag [110] row in linear density (difference  $\sim 0.5\%$ ) and hence expected to be stable; whereas the pseudomorphic lines are too dense or too sparse. The pseudomorphic lines are calculated with the  $6 \times 2$  cell ( $1 \times 6$   $k$ -point grid), and the CSL line with the  $6 \times 6$  cell ( $1 \times 2$   $k$ -point grid); here, the  $1 \times 1$  cell denotes the primitive cell of the ideal Si(001) surface. Energies obtained with these two different cells can be directly compared: the total energy (per  $6 \times 2$  cell) of the interior monomer line (see figure 3(a)) obtained with the  $6 \times 6$  cell differs by no more than 0.5 meV from that obtained with the  $6 \times 2$  cell. As in [16], the energetic stability of an Ag line is expressed in terms of the adsorption potential energy ( $E_a$ ) calculated according to

$$E_a = (E - E_0)/n - \varepsilon_{\text{Ag}}, \quad (1)$$

where  $E$  is the total energy,  $E_0$  is the energy of the substrate,  $n$  is the number of Ag atoms, and  $\varepsilon_{\text{Ag}}$  is the energy of a free, spin polarized Ag atom. In this definition, low  $E_a$  indicates greater energetic stability.

<sup>1</sup> Simulation Tool for Atom TEchnology (STATE) Ver. 5.01, Research Institute for Computational Sciences (RICS), National Institute of Advanced Industrial Science and Technology (AIST), 2002.

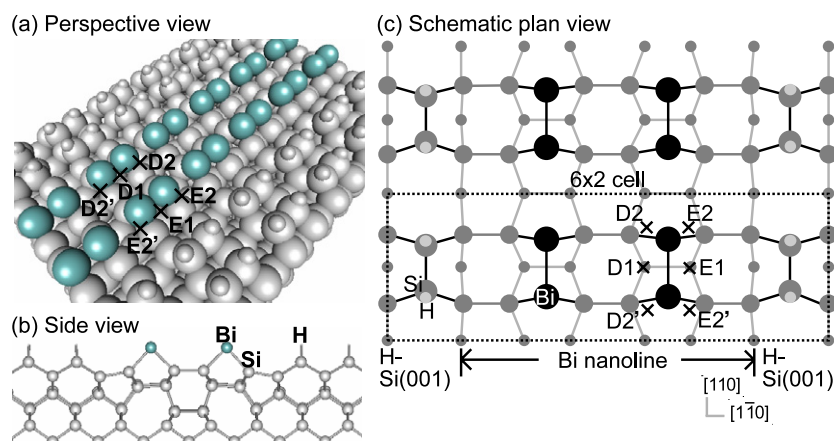


**Figure 1.** Model of the H-terminated Si(001) surface featuring a Bi nanoline. Interior (D1, D2, D2') and exterior (E1, E2, E2') back-bond sites [16] are indicated. Equivalent sites are distinguished by apostrophes.

**Table 1.** Difference  $\Delta E$  (eV) of  $E_a$  between the registered and staggered dimer lines (see figures 5(b) and (c)) calculated at various conditions.  $N_l$  denotes the number of atomic layers in the slab.  $E_{\text{cut}}$  (Ryd) denotes the cut-off energy.

Cell	$N_l$	$k$ point	$E_{\text{cut}}$	$\Delta E$	
$6 \times 2$	6	$1 \times 6$	16	0.027	Present (short cell)
$6 \times 2$	6	$1 \times 6$	<b>20</b>	0.027	Higher cut-off
$6 \times 2$	6	$1 \times 8$	16	0.027	More $k$ points
$8 \times 2$	<b>8</b>	$1 \times 6$	16	0.028	Larger model

The accuracy of the calculation has been ascertained by calculating the difference of  $E_a$  between two types of double dimer lines (see figures 5(b) and (c)) at various conditions (table 1). The energy difference is changed little ( $\sim 0.001$  eV) by the increase in the cut-off energy, the number of  $k$  points, and the size of the slab model. Thus, energy differences of  $\sim 0.01$  eV can be discussed.

### 3. Results and discussion

#### 3.1. Exterior Ag lines

If the temperature is such that Ag can migrate on the H-terminated Si(001) surface (barrier  $\sim 0.14$  eV) to a Bi nanoline but cannot enter its interior (barrier  $\sim 0.53$  eV), then Ag adsorbs on its exterior. To ascertain whether this leads to the growth of atomic Ag lines, we examine the Ag lines shown in figure 2.

Figures 2(a)–(c) show pseudomorphic lines where Ag occupies exterior back-bond sites (E1, E2, and E2' in figure 1). In figure 2(a), Ag occupies E1, the most stable site [16] on the exterior, forming a monomer line. The calculated band structure shows a slightly dispersive band crossing the Fermi level, indicating a non-negligible interaction among the monomers. In figure 2(b), Ag occupies E1 and E2, forming a dimer line. The Ag–Ag bond length (0.282 nm) is close to the calculated bulk value (0.289 nm). The dimer line has a large energy gap (0.64 eV) and gains energy over the monomer line, as expected from the formation of dimer bonds. In

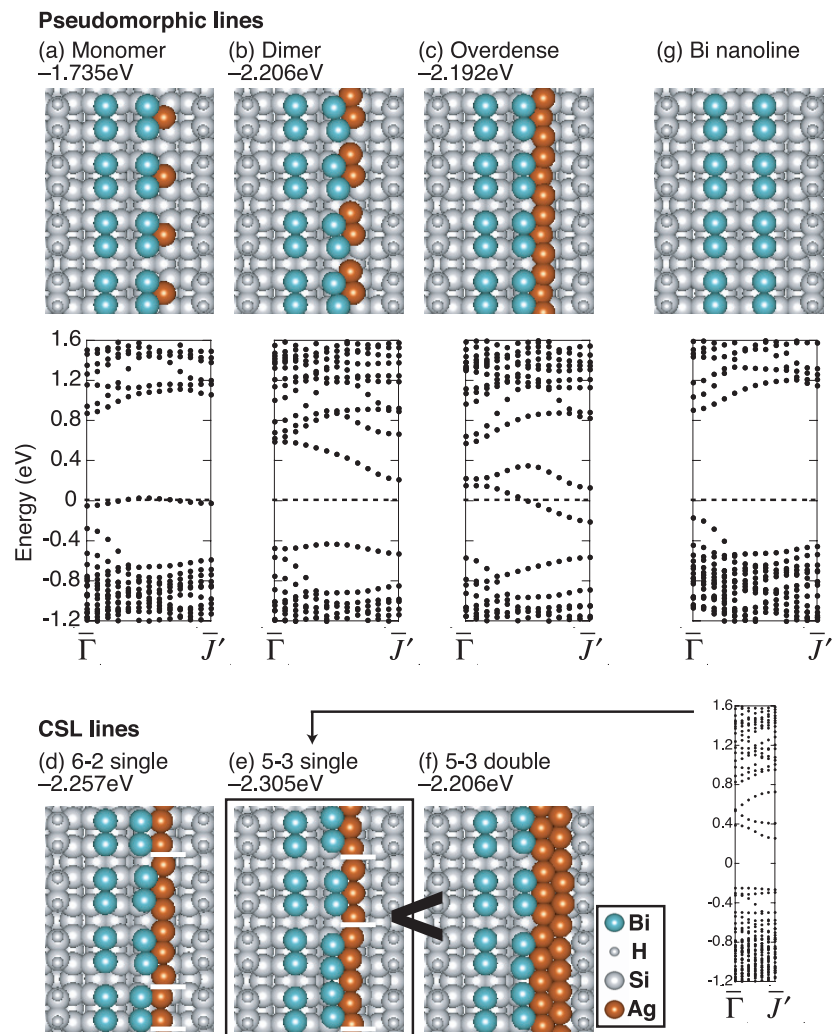


**Figure 2.** (a)–(f) Ag lines on the exterior of the Bi nanoline (plan view). Optimized geometries and calculated energies  $E_a$  (eV) are shown. In (d) and (e), the pattern is indicated by white lines. The inequality sign indicates the greater stability of the single-row CSL line against the double-row one. (g) The Bi nanoline (plan view). For (a)–(c), (e), and (g), the calculated band structure along the line direction ( $\Gamma J'$ ) is shown. The Fermi level is at zero energy.

figure 2(c), Ag occupies E1, E2, and E2', forming a continuous line with a linear density exceeding that of the bulk Ag [110] row by 12%. This overdense line, although having two Ag–Ag bonds per Ag atom, is only as stable as the dimer line; the shortening of the Ag–Ag bonds (to 0.265–0.266 nm) can be energetically unfavourable. Its band structure is metallic, with a half-filled band inside the energy gap of the substrate.

Figures 2(d) and (e) show two types of single-row CSL lines: in the '6–2' pattern (figure 2(d)), six of the eight Ag atoms match two Bi dimers, and the other two match a Bi dimer; whereas in the '5–3' pattern (figure 2(e)), five Ag atoms match two Bi dimers, and the other three match a Bi dimer. The 5–3 line is found more stable than the 6–2 line, as expected from the fact that the former has the Ag atoms distributed more evenly among the Bi

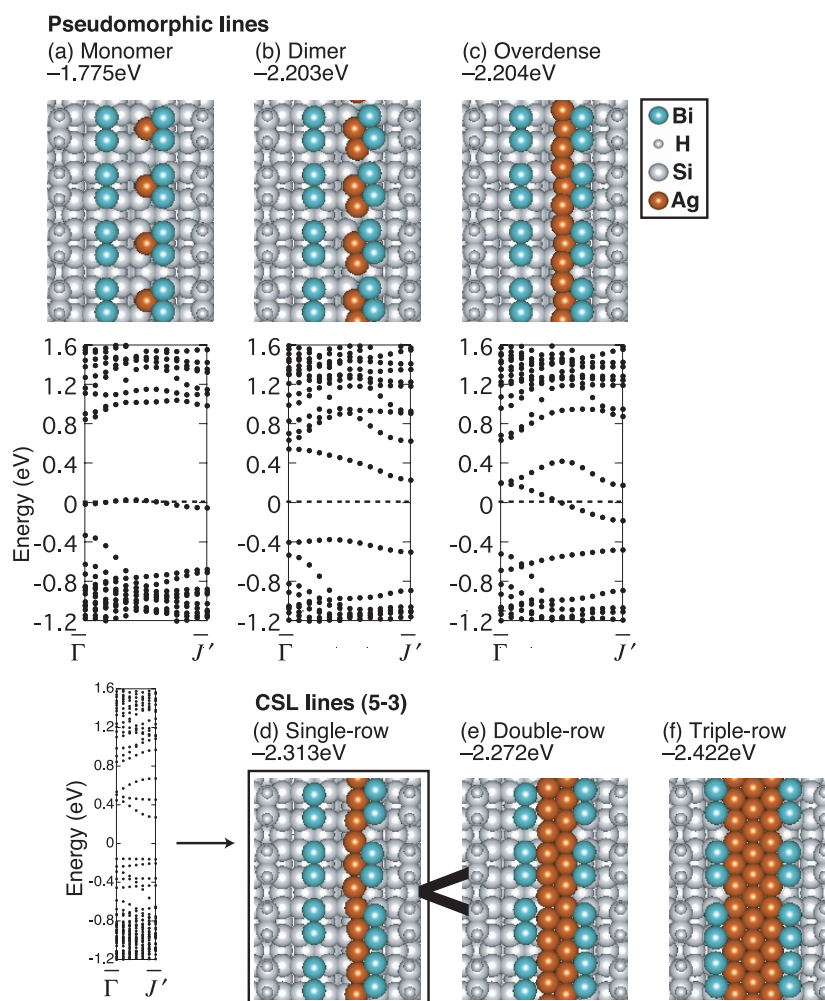


**Figure 3.** Single Ag lines on the interior of the Bi nanoline (plan view). Optimized geometries and calculated energies  $E_a$  (eV) are shown. For (a)–(d), the calculated band structure along the line direction ( $\Gamma$ – $J'$ ) is also shown. The inequality sign indicates the greater stability of the single-row CSL line against the double-row one.

dimers (2.5, 2.5, and 3 atoms) than the latter does (3, 3, and 2 atoms). (Thus, the 6–2 pattern is not considered below.) As expected from the excellent lattice match with the Bi nanoline template, the CSL line is found to have a lower energy than the overdense line; in fact, the lowest among the single lines calculated here (figures 2(a)–(e)). Moreover, the single-row CSL line is more stable than the double-row one (figure 2(f)) that grows out of the back-bonds. Thus, the energetic stability improves as we go from the monomer line (figure 2(a)) to the dimer line (figure 2(b)) to the CSL line (figure 2(e)), but further increase in linear density (figure 2(c)) or the growth out of the back-bonds (figure 2(f)) is energetically unfavourable. This trend indicates the feasibility of single-row Ag lines, in particular, the CSL line.

The CSL line has a semiconducting band structure (figure 2(e)). The small energy gap (0.5 eV) compared to that (1.1 eV) of the Bi nanoline (figure 2(g)) indicates the possibility that the CSL line becomes a conducting wire under doping.



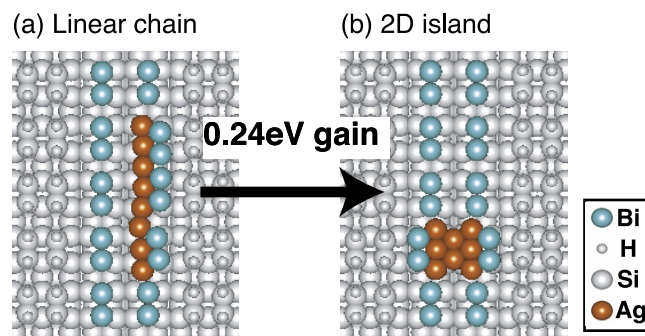


**Figure 4.** Optimized geometries of  $\text{Ag}_8$  clusters (plan view). The triple-row structure (b) is 0.24 eV (per cluster) more stable than the single-row one (a).

### 3.2. Interior Ag lines

In the previous section, we have examined the Ag lines on the exterior of the Bi nanoline and found that the single-row CSL line is feasible. This is relevant when the temperature is too low to allow Ag to enter inside the Bi nanoline. In this section, on the other hand, we examine Ag lines on the interior, supposing that the temperature is sufficiently high. We again find the single-row CSL line to be particularly stable, but not as stable as the triple-row one. In addition, we examine double Ag lines where Ag is adsorbed on both branches of the Bi nanoline and find that they are less stable than the CSL single line.

**3.2.1. Single lines.** Figure 3 shows Ag lines on the interior of the Bi nanoline. As in section 3.1, we examine the pseudomorphic lines where Ag occupies back-bond sites (D1, D2, and D2' in figure 1), as well as the CSL line (in the 5–3 pattern). The energetic stability improves as we go from the monomer line (figure 3(a)) to the dimer line (figure 3(b)) to the single-row CSL line (figure 3(d)), but worsens if we go further to the overdense line (figure 3(c)) or to the double-row CSL line (figure 3(e)). This trend again indicates the feasibility of the single-row CSL line, as expected from its excellent lattice match and the favourableness of residing in the back-bonds. This interior CSL line has a band structure (figure 3(d)) similar to that of the exterior one (figure 2(e)).

However, the double-row CSL line (figure 3(e)) is rather stable and hence close in energy to the single-row one; in contrast to its exterior counterpart, the second Ag row is close enough (0.30 nm) to the other branch of the Bi nanoline to gain energy due to Ag–Bi interaction (Ag–Bi bonds are  $\sim 0.28$  nm long [16]). Moreover, the triple-row CSL line (figure 3(f)) is more stable than the single-row one<sup>2</sup>. This energy ordering suggests that triple-row islands can be more stable than linear chains.

This point is illustrated in figure 4 by using  $\text{Ag}_8$  clusters as an example. (The  $6 \times 8$  cell and the  $1 \times 2$   $k$ -point grid were used in calculating these clusters.) The greater stability of the 2D island (figure 4(b)) against the linear chain (figure 4(a)) indicates that linear chains are prone to transform into islands. Thus, a low temperature must be used for the growth of single-row lines, either to suppress such transformation or to prevent Ag from entering inside the Bi nanoline (barrier  $\sim 0.53$  eV [16]).

<sup>2</sup> This Ag(111) monolayer with the 5–3 pattern is found slightly more stable than that with the 6–2 pattern examined in [17].

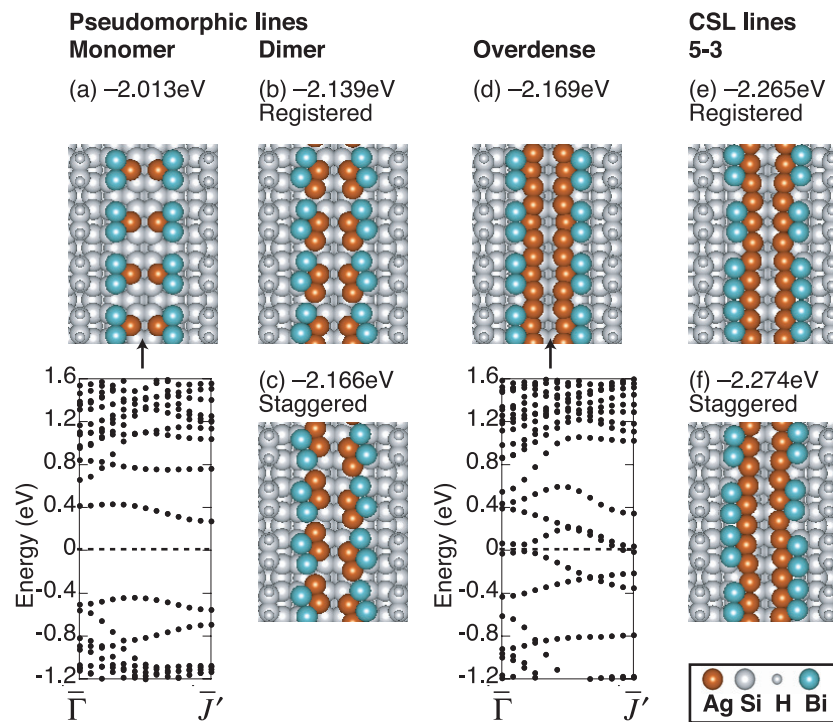


**Figure 5.** Double Ag lines (plan view). Optimized geometries and calculated energies  $E_a$  (eV) are shown. For (a) and (d), the calculated band structure along the line direction ( $\Gamma J'$ ) is also shown. The Fermi level is at zero energy.

**3.2.2. Double lines.** Now we examine double lines (figure 5) where Ag is adsorbed on both branches of the Bi nanoline. We examine the interaction between the two branches and find that the double lines are less stable than the CSL single line.

The double monomer line (figure 5(a)) is far more stable than the single monomer line (figure 3(a)); the half-filled bands of the single lines split into filled and empty bands separated 0.7 eV, thus gaining energy. This line is however still high in energy compared to the others.

The double dimer line (figures 5(b) and (c)), in contrast, is expected to experience repulsion between filled bands because the single line has an energy gap (figures 3(b)). Accordingly, the double line is found less stable than the single line, whether the Ag dimers are registered (figures 5(b)) or staggered (figures 5(c)). The slight metastability of the registered one against the staggered one also indicates the repulsion between the two branches. Similarly, the CSL double line is less stable than the single line, whether the two branches are registered (figure 5(e)) or staggered (figure 5(f)). The latter is however almost as stable as the double-row line (figure 3(e)). This degeneracy indicates that the energy punishment of leaving the back-bonds is at least comparable to the energy gain of bonding between two Ag rows.

The overdense double line (figure 5(d)), on the other hand, has a metallic band structure; the half-filled bands of the single lines (figure 3(c)) do not completely split into filled and empty bands because their dispersion is large. Hence, a large energy gain may not be expected. The double line is actually found less stable than the single line. Thus, none of the double lines examined here is more stable than the CSL single line.



#### 4. Conclusions

The energetic stability of Ag lines epitaxial to the Bi nanoline has been examined at the GGA level. For the exterior Ag lines, we have found that the stability improves as we go from the monomer line to the dimer line to the single-row CSL line, but worsens if we go further to the overdense line or to the double-row CSL line. This trend indicates the feasibility of single-row lines, in particular, the CSL line. The calculated band structure indicates that the CSL line is semiconducting. For the interior Ag lines, the same energy ordering has been found. The greater stability of the triple-row CSL line however suggests that triple-row islands can be more stable than linear chains. This has been found for the  $\text{Ag}_8$  cluster. Thus, a low temperature should be used for the growth of the Ag lines, either to prevent Ag from entering inside the Bi nanoline or to suppress the transformation from linear chains into islands. Kinetics simulations using the barriers given in [16] may be useful in finding such conditions.

#### Acknowledgments

The calculations were performed on the Numerical Materials Simulator at NIMS and on the NEC SX-5 at Cyber Media Centre, Osaka University. HK is supported by the JSPS. This work is in part supported by a Grant-in-Aid from the Ministry of Education, Culture, Sports, Science and Technology.

#### References

- [1] Bowler D R 2004 *J. Phys.: Condens. Matter* **16** R721
- [2] Lyding J W, Shen T C, Hubacek J S, Tucker J R and Abeln G C 1994 *Appl. Phys. Lett.* **64** 2010
- [3] Lyding J W, Abeln G C, Shen T C, Wang C and Tucker J R 1994 *J. Vac. Sci. Technol. B* **12** 3735
- [4] Shen T C, Wang C, Abeln G C, Tucker J R, Lyding J W, Avouris P and Walkup R E 1995 *Science* **268** 1590
- [5] Hitosugi T, Hashizume T, Heike S, Watanabe S, Wada Y, Hasegawa T and Kitazawa K 1997 *Japan. J. Appl. Phys.* **2** **36** L361
- [6] Hashizume T, Heike S, Lutwyche M I, Watanabe S, Nakajima K, Nishi T and Wada Y 1996 *Japan. J. Appl. Phys.* **2** **35** L1085
- [7] Hashizume T, Heike S, Lutwyche M I, Watanabe S and Wada Y 1997 *Surf. Sci.* **386** 161
- [8] Sakurai M, Thirstrup C and Aono M 2000 *Phys. Rev. B* **62** 16167
- [9] Miki K, Bowler D R, Owen J H G, Briggs G A D and Sakamoto K 1999 *Phys. Rev. B* **59** 14868
- [10] Naitoh M, Shimaya H, Nishigaki S, Oishi N and Shoji F 1997 *Surf. Sci.* **377–379** 899
- [11] Bowler D R and Owen J H G 2002 *J. Phys.: Condens. Matter* **14** 6761
- [12] Owen J H G and Miki K 2006 *Nanotechnology* **17** 430
- [13] Bowler D R, Bird C F and Owen J H G 2006 *J. Phys.: Condens. Matter* **18** L241
- [14] Owen J H G and Miki K 2006 *Surf. Sci.* **600** 2943
- [15] Orellana W and Miwa R H 2006 *Appl. Phys. Lett.* **89** 093105
- [16] Koga H and Ohno T 2006 *Phys. Rev. B* **74** 125405
- [17] Koga H and Ohno T 2007 *J. Phys.: Condens. Matter* **19** to appear in the special issue Proceedings of the International Conference on Quantum Simulators and Design
- [18] Hohenberg P and Kohn W 1964 *Phys. Rev.* **136** B864
- [19] Kohn W and Sham L J 1965 *Phys. Rev.* **140** A1133
- [20] Vanderbilt D 1990 *Phys. Rev. B* **41** 7892
- [21] Troullier N and Martins J L 1991 *Phys. Rev. B* **43** 1993
- [22] Perdew J P, Burke K and Ernzerhof M 1996 *Phys. Rev. Lett.* **77** 3865